# Ion−Molecule Reactions of Gas-Phase Chromium Oxyanions: $Cr_xO_yH_z^- + H_2O$

**A. K. Gianotto, B. D. M. Hodges, M. T. Benson, P. de B. Harrington,† A. D. Appelhans, J. E. Olson, and G. S. Groenewold***

*Idaho National Engineering and Environmental Laboratory, Idaho Falls, Idaho 83415-2208*

*Received: September 26, 2002; In Final Form: February 18, 2003*

Chromium oxyanions having the general formula $Cr_xO_yH_z^-$ play a key role in many industrial, environmental, and analytical processes, which motivated investigations of their intrinsic reactivity. Reactions with water are perhaps the most significant, and were studied by generating $Cr_xO_yH_z^-$ in the gas phase using a quadrupole ion trap secondary ion mass spectrometer. Of the ions in the $Cr_1O_yH_z$ envelope ($y = 2, 3, 4$; $z = 0, 1$), only $CrO_2^-$ was observed to react with $H_2O$, producing the hydrated $CrO_3H_2^-$ at a slow rate (~0.07% of the ion−molecule collision constant at 310 K). $CrO_3^-$, $CrO_4^-$, and $CrO_4H^-$ were unreactive. In contrast, $Cr_2O_4^-$, $Cr_2O_5^-$, and $Cr_2O_5H_2^-$ displayed a considerable tendency to react with $H_2O$. $Cr_2O_4^-$ underwent sequential reactions with $H_2O$, initially producing $Cr_2O_5H_2^-$ at a rate that was ~7% efficient. $Cr_2O_5H_2^-$ then reacted with a second $H_2O$ by addition to form $Cr_2O_6H_4^-$ (1.8% efficient) and by OH abstraction to form $Cr_2O_6H_3^-$ (0.6% efficient). The reactions of $Cr_2O_5^-$ were similar to those of $Cr_2O_5H_2^-$: $Cr_2O_5^-$ underwent addition to form $Cr_2O_6H_2^-$ (3% efficient) and OH abstraction to form $Cr_2O_6H^-$ (<1% efficient). By comparison, $Cr_2O_6^-$ was unreactive with $H_2O$, and in fact, no further $H_2O$ addition could be observed for any of the $Cr_2O_6H_z^-$ anions. Hartree−Fock ab initio calculations showed that reactive $Cr_xO_yH_z^-$ species underwent *nucleophilic* attack by the incoming $H_2O$ molecules, which produced an initially formed adduct in which the water O was bound to a Cr center. The experimental and computational studies suggested that $Cr_2O_yH_z^-$ species that have bi- or tricoordinated Cr centers are susceptible to attack by $H_2O$; however, when the metal becomes tetracoordinate, reactivity stops. For the $Cr_2O_yH_z^-$ anions the lowest energy structures all contained rhombic $Cr_2O_2$ rings with pendant O atoms and/or OH groups. The initially formed $[Cr_2O_y^- + H_2O]$ adducts underwent H rearrangement to a *gem* O atom to produce stable dihydroxy structures. The calculations indicated that rearrangement did not occur in the $[Cr_2O_5H_2^- + H_2O]$ adduct, possibly because the rearranged product could not accommodate the negative charge.

## I. Introduction

The reactions of chromium oxyanions with water influence chromium speciation, which in turn affects the reactivity of the resultant species. Altered Cr speciation can result in biological and environmental toxicity, and increased mobility in the lithosphere,[1−3] which is normally associated with exacerbated environmental risk.[4−9] The acute significance of species-dependent chromium toxicity has resulted in a sustained emphasis within the research community to perform sensitive speciation determinations on contaminated mineral surfaces.[6,9−16] Desorption ionization mass spectrometry, using either laser pulses[10,14,16−26] or particle impacts,[23,27−29] has received particular attention because of the potential for high selectivity and sensitivity.

Desorption ionization of chromium oxide-bearing surfaces produces abundant ions having the general formula $Cr_xO_yH_z^{+/-}$.[27] The ions observed, and their relative abundances, vary depending on the species being examined. Determination of chromium speciation relies on correlating the observed ions and their abundance with the chemical form of chromium as it originally existed on the mineral surface. This becomes complicated by the occurrence of ion−molecule reactions, both aggregative and dissociative, that occur in the gas phase both during and after the surface irradiation event. The influence of the ion−molecule reactions on observed $Cr_xO_yH_z^-$ was noted by Muller and co-workers in a recent investigation of Cr speciation using laser desorption.[17] Water in particular was suspected to be responsible for oxidizing Cr secondary ions observed in desorption ionization mass spectra.[20,21] Water is a potential participant in ion formation processes, because it adheres to all metal oxide surfaces, and will partition between the surface and the gas phase in a vacuum environment. Because desorption ionization involves both the surface and the gas phase, water has the opportunity to participate in reactions with nascent ions being sputtered from the surface. Hence, an explicit understanding of the role that adventitious water plays in influencing the suite of $Cr_xO_yH_z^-$ ions observed in a desorption-ionization-type analysis would be beneficial.

From a more fundamental perspective, a detailed inventory of chromium oxyanion reactivity with water would provide insight into the types of moieties likely to influence hydrolysis reactions occurring under ambient conditions. Generally, undercoordinated metal or metalloid edge sites are thought to be aggressive participants in hydrolysis and cation adsorption processes.[30−32] In principle it should be possible to mimic hydrolysis and adsorption processes using gas-phase metal oxycations and anions because low-coordinate $M_xO_y$ ions can be easily formed by particle or photon desorption in some systems.[32] Surfaces that form abundant metal oxyanions upon surface irradiation tend to contain transition metals from groups

† Clippinger Labs, Ohio University Center for Intelligent Chemical Instrumentation, Athens, OH 45701-2979.

* Corresponding author.

10.1021/jp027083l CCC: $25.00 
Published on Web 07/11/2003

VB, VIB, and VIIB. In addition to the Cr oxyanions cited above, gas-phase $M_xO_y^-$ ions have been generated starting from oxides of V, Mo, W, Mn, and Re.[32−40] But little is known about the reactions of the transition-metal oxyanions with $H_2O$, other than the work of Dinca and co-workers, who showed that four different $V_xO_y^-$ ($x = 1-3$) ions would undergo adduct formation.[32] Their work demonstrated that water reactivity with metal oxyanions was readily investigatable using trapped ion mass spectrometry combined with desorption ionization (laser desorption Fourier transform ion cyclotron resonance mass spectrometry).[32] An alternative instrumental approach that has been employed in our laboratory utilizes an ion trap secondary ion mass spectrometer (IT-SIMS); in this technique, ions are produced by bombarding metal oxide-bearing surfaces with energetic ions, and the sputtered $M_xO_y^-$ ions are isolated, reacted, and analyzed using a quadrupole ion trap.

Using the IT-SIMS, the reactions of Al and Si oxyanions with $H_2O$ were investigated. Sequential dissociative addition occurred until tetracoordinate Si and Al product ions were finally formed,[41,42] after which further addition reactions were not observed in the $1 \times 10^{-4}$ Torr He atmosphere of the ion trap. Ab initio calculations showed that $M_2O_yH_z^-$ (M = Al or Si) possessed rhombic $M_2O_2$ moieties, and that the initial adducts were formed as a result of H-bonding with pendant O atoms, which carried the negative charge. The adducts then rearranged to form covalently bound, hydroxylated products. No evidence for the formation of stable, noncovalent water cluster anions was apparent. The Si and Al studies also showed dramatic differences in reactivity stemming from apparently subtle differences in ion composition and structure. For example, the reactivity of $M_2O_yH_z^-$ (M = Al or Si) was 1−2 orders of magnitude greater than that of $M_1O_yH_z^-$. Ab initio calculations suggested that this difference was due to low-lying transition states available to $Si_2O_xH_z^- + H_2O$ systems that were not available to $Si_1O_yH_z^-$ ions, but did not provide a satisfactory explanation for the Al systems, in which transition states for $Al_1O_yH_z^-$ species were comparable to those for $Al_2O_yH_z^-$. These initial Al−Si oxyanion studies demonstrated the utility of the IT-SIMS for describing the phenomenology of metal oxyanion reactivity behavior and provided a basis of comparison for the present $Cr_xO_yH_z^-$ studies.

In the present study, the gas-phase reaction pathways of $Cr_xO_yH_z^- + H_2O$ were elucidated at ion temperatures typical of an ion trap (310 K). Relative reactivity was compared by evaluating rate constants, and insight into the structural and thermodynamic aspects of the salient reactions was generated using ab initio calculations.

## II. Experimental Section

**IT-SIMS Experiments.** Gas-phase $Cr_xO_y^-$ species were produced by bombarding powdered potassium dichromate (Baker Chemical, Phillipsburg, NJ) that was attached (double-sided tape, 3M, St. Paul, MN) to the end of a 2.7 mm probe tip. The sputtered $Cr_xO_yH_z^-$ ions were then trapped in the IT-SIMS, where they were reacted with $H_2O$, which was admitted to the vacuum chamber in the following manner: 18 MΩ demineralized $H_2O$ was subjected to freeze−pump−thaw cycles to eliminate contaminant gases. A variable leak valve was then used to control the admittance of $H_2O$ vapor into the IT-SIMS for ion−molecule reaction experiments. $H_2O$ pressures in the ion−molecule experiments were $\sim(1-2) \times 10^{-6}$ Torr. Because the ion gauge response for $H_2O$ is nearly identical to $N_2$, ion gauge pressures were used without correction.[43] The helium bath gas was operated at a pressure of $1 \times 10^{-4}$ Torr (corrected for ion gauge sensitivity); since the ion trap has a fairly open design, we believe that this is close to the He pressure within the ion trap. The IT-SIMS base pressure was $\sim 5 \times 10^{-8}$ Torr.

The IT-SIMS[44] is a modified Finnigan ITMS instrument (Finnigan Corp., San Jose, CA) that incorporated a perrhenate ($ReO_4^-$) primary ion beam, an insertion lock for introduction of solid samples, and an offset dynode with a multichannel plate detector. The primary ion gun and sample probe tip are collinear and located outside opposite end caps of the ion trap. The primary ion gun was operated at 4.5 keV and produced a $ReO_4^-$ beam with a 1.25 mm diameter at a primary ion current ranging from 300 to 450 pA. The $ReO_4^-$ beam was used because this type of ion beam is more efficient for sputtering larger cluster ions into the gas phase than atomic particle bombardment.[29,45,46] The data acquisition and control system uses the Teledyne Apogee ITMS Beta Build 18 software that controls routine ITMS functions and a filtered noise field (FNF) system (Teledyne Electronic Technologies, Mountain View, CA). Data analysis was performed using SATURN 2000 software (version 1.4, Varian, Walnut Creek, CA).

The sequence of events for conducting ion−molecule reactivity experiments is similar to that utilized in earlier studies.[42] Ionization times were adjusted to produce an acceptable number of ions (signal-to-noise ratio $\geq \sim 100$) for reactivity experiments. During ionization the $ReO_4^-$ beam was directed through the ion trap and onto the chromium oxide target. The ion trap was operated with a low mass cutoff of 40 amu. Ion isolation was performed at the same time as ionization (sample bombardment) by applying an FNF. The FNF, in which white noise at millivolt levels is applied to the ion trap end caps, allows for mass-selective ejection of ions whose mass-dependent motional frequencies fall outside a set $m/z$ range.[47] The width of the $m/z$ range is adjustable using the FNF; however, there is a tradeoff of selectivity versus abundance; i.e., ion abundance can decrease in some instances where a high degree of selectivity is needed. We strove to keep the abundances at adjacent masses <5% of the abundance of the selected reactant ion.

Once the specified ions were formed, trapped, and isolated, the progress of the reactions with $H_2O$ was followed by altering the duration of a delay period between the ionization/isolation event and the ion scan-out/detection event. After reaction, ions were scanned out of the ion trap using a mass-selective instability scan with axial modulation.[48] Background spectra were collected for each sample by retracting the sample probe sufficiently to eliminate ion formation from the target. Seven spectra (each composed of the average of 20 scans) were averaged and background subtracted to obtain final peak intensities. The relative standard deviation between averaged spectra was ±5%.

**Computational Methods.** Calculations were performed using the General Atomic and Molecular Electronic Structure System (GAMESS)[49] quantum chemistry program at the Hartree−Fock (HF) level of theory. The calculations utilized the 3-21G split valence basis set with diffuse sp and d shells added to oxygen. Effective core potentials were not used in any of the calculations, so all structures are full electron. Vibrational frequencies were calculated for all HF-optimized geometries to ensure that the transition states had only one imaginary frequency and all other minima had zero imaginary frequencies. Intrinsic reaction coordinate (IRC) calculations[50,51] were performed on all transition states at the HF level of theory to ensure that the reactants, transition states, and products occurred on the same reaction path. To include correlation contributions, single-point energies were calculated with the Møller−Plesset second-order perturba-

tion theory (MP2)[52] for each HF-optimized geometry. Energies were corrected using the zero-point energies and from absolute zero to 298.15 K using HF vibrational frequencies. Thermodynamic data calculated have been shown to agree well with experiment for a variety of transition-metal reactions, especially for related complexes and reactions.[53−59] Without experimental data to compare against, an error for calculated thermodynamic data cannot be determined; however, on the basis of previous transition-metal calculations cited, relative energies between structures having similar compositions are expected to be adequate.

**Calculation of Rate Constants.** The reactions of the isolated $Cr_xO_yH_z^-$ species with $H_2O$ were measured directly and were described using pseudo-first-order kinetics. A pseudo-first-order approximation was appropriate because the concentration of $H_2O$ was significantly greater than the concentration of the ions, and hence, the $H_2O$ concentration remained constant throughout the reaction. Uncertainty in the accuracy of the $H_2O$ concentration, especially at low pressure, was felt to be the principle contributor to the uncertainty of the rate constant calculations. Experiments repeated at about equivalent $H_2O$ pressures gave rate constants that varied ±20% relative.

The reactions examined were accurately described using pseudo-first-order kinetics, as if they were bimolecular. However, collisions with the He bath gas, which are needed in an ion trap to damp ion trajectories, certainly serve to collisionally stabilize initially formed adducts, effectively making the reactions termolecular.[60] Since rates for vibrational cooling tend to be slow,[61] alternative stabilization mechanisms such as radiative association may be operative.[62] At any rate, the narrow range of operating pressures for trapping the anions in the IT-SIMS ($(2-5) \times 10^{-5}$ Torr gauge) did not facilitate an extensive evaluation of the role of the He bath gas in these reactions. Over the range of accessible He pressures, significant variations in the measured reaction rates were not observed. This suggested that the initially formed adducts were not particularly sensitive to stabilization by thermal collisions with He. For this reason, the reactions were described using bimolecular rate constants.[60,63]

$CrO_2^-$, $Cr_2O_4^-$, and $Cr_2O_5^-$ all underwent a combination of consecutive and parallel reactions, which made assignment of reaction pathways and calculation of individual rate constants difficult. A multivariate curve resolution (MCR) approach[64] was employed to identify reaction pathways in an unbiased fashion. Reactant and product ion relationships and their general kinetic behavior were determined using the MCR method SIMPLISMA.[65] Next, a hard-modeling approach that used an alternating least-squares (ALS) regression[66,67] was employed to generate concentration profiles starting from the MCR-derived kinetic model. Finally, a set of kinetic rate equations were fit to the concentration profiles obtained from ALS using the MATLAB 6.1 (Mathworks, Inc., Natick, MA) function FMINSEARCH, which uses a nonlinear simplex optimization.[68] This method, referred to as the ALS method in this paper, was used because it eliminated bias in the assignment of reaction pathways and provided reaction rates that were optimized to the actual data sets. A comprehensive description of the method is in preparation.[64]

Reaction efficiency was evaluated by comparing measured rate constants with theoretical rate constants calculated using the reparametrized average-dipole-orientation (ADO) theory.[69] The reparametrized ADO constants were calculated using a reaction temperature (310 K) which was the average ion temperature for an ion in a typical trap as calculated by both Goeringer[70] and Gronert.[71]

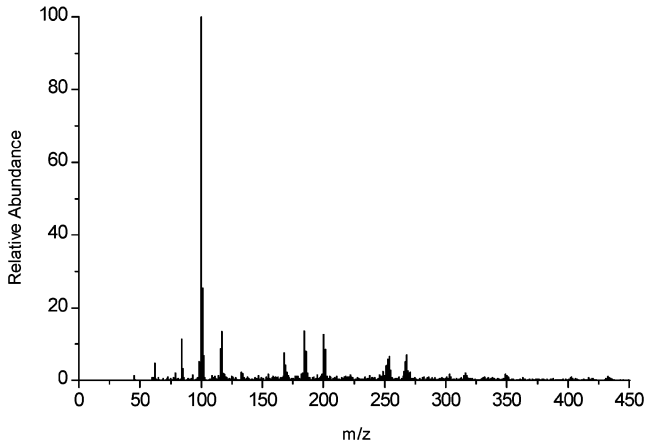


**Figure 1.** Anion IT-SIMS spectra of potassium dichromate. Ion envelopes corresponding to $Cr_1O_yH_z^-$ are observed between *m*/*z* 84 and *m*/*z* 117, $Cr_2O_yH_z^-$ between *m*/*z* 168 and *m*/*z* 200, and $Cr_3O_yH_z^-$ between *m*/*z* 252 and *m*/*z* 268.

## III. Results and Discussion

The negative secondary ion mass spectra of chromium(VI) oxide species acquired using the IT-SIMS (Figure 1) qualitatively resembled laser desorption[21] and SIMS[27] mass spectra previously reported, in that envelopes of abundant ions having the general formulas $Cr_1O_yH_z^-$ and $Cr_2O_yH_z^-$ were observed. In the $Cr_1O_yH_z^-$ envelope, the significant anions and compositions were *m*/*z* 84 ($CrO_2^-$), 100 ($CrO_3^-$), 116 ($CrO_4^-$), and 117 ($HCrO_4^-$). In the $Cr_2O_yH_z^-$ envelope, the significant ions were *m*/*z* 168 ($Cr_2O_4^-$), 184 ($Cr_2O_5^-$), 185 ($Cr_2O_5H^-$), 200 ($Cr_2O_6^-$), and 201($Cr_2O_6H^-$), and in the $Cr_3O_yH_z^-$ envelope, *m*/*z* 252 and 268 corresponded to $Cr_3O_6^-$ and $Cr_3O_7^-$, respectively.

The reactions of the chromium oxyanions with $H_2O$ were studied by establishing a constant water concentration in the ion trap, and then isolating the ion of interest. All of the $Cr_1$ species were studied, as were $Cr_2O_4^-$, $Cr_2O_5^-$, and $Cr_2O_6^-$. The H-bearing $Cr_2$ species and the $Cr_3$ species were not examined because they were sensitive to primary ion dose and it was difficult to maintain satisfactory abundance of these isolated ions.

**$Cr_1O_yH_z^- + H_2O$.** Four ions were evaluated for reaction with $H_2O$, viz., $CrO_2^-$, $CrO_3^-$, $CrO_4^-$, and $CrO_4H^-$. Of these, only $CrO_2^-$ displayed a measurable reaction over 2 s, which was the maximum allowed by the instrument control software for a single ionization/reaction/scan-out sequence. Isolation of $CrO_2^-$ (*m*/*z* 84) followed by reaction with $H_2O$ appeared to result in the formation of $CrO_3^-$ at *m*/*z* 100 (Supporting Information); however, later experiments in which $O_2$ was the dominant reactant gas in the IT-SIMS strongly indicated that the $CrO_3^-$ product ion was due to reaction with background $O_2$, and not $H_2O$. This conclusion was substantiated by ab initio calculations, which failed to find a transition state for the reaction $CrO_2^- + H_2O$.

In addition to the appearance of $CrO_3^-$, however, a lower abundance ion was also observed at *m*/*z* 102, which corresponded to $CrO_3H_2^-$. The kinetic profile (Supporting Information) indicated that the reactions with $H_2O$ and $O_2$ were occurring in parallel and did not support sequential reactions for formation of $CrO_3^-$ (i.e., addition of $H_2O$ followed by slower expulsion of $H_2$). ALS evaluation of the rate constant (Table 1) showed that the reaction was slow and inefficient, ~0.07% of

**TABLE 1: Rate Constants and Efficiencies for Cr Oxyanions Reacting with $H_2O$**

| (eq no.) reaction | reactant *m/z* | product *m/z* | $k_{individual}$[a,b] | $k_{ADO}$[a,c] | reaction efficiency[d] (%) |
|---|---|---|---|---|---|
| | | $Cr_1O_yH_z^-$ | | | |
| $CrO_2^- + H_2O \rightarrow CrO_3H_2^-$ | 84 | 102 | $2 \times 10^{-12}$ | $2.3 \times 10^{-9}$ | 0.1 |
| $CrO_3^- + H_2O \rightarrow$ no reaction | 100 | no reaction[e] | | $2.2 \times 10^{-9}$ | |
| $CrO_4^- + H_2O \rightarrow$ no reaction | 116 | no reaction[e] | | $2.2 \times 10^{-9}$ | |
| $CrO_4H^- + H_2O \rightarrow$ no reaction | 117 | no reaction[e] | | $2.2 \times 10^{-9}$ | |
| | | $Cr_2O_yH_z^-$ | | | |
| (1) $Cr_2O_4^- + H_2O \rightarrow Cr_2O_5H_2^-$ | 168 | 186 | $1 \times 10^{-10}$ | $2.2 \times 10^{-9}$ | 7 |
| (2) $Cr_2O_5H_2^- + H_2O \rightarrow Cr_2O_6H_3^- + H$ | 186 | 203 | $1 \times 10^{-11}$ | $2.2 \times 10^{-9}$ | 0.6 |
| (3) $Cr_2O_5H_2^- + H_2O \rightarrow Cr_2O_6H_4^-$ | 186 | 204 | $4 \times 10^{-11}$ | $2.2 \times 10^{-9}$ | 2 |
| (4) $Cr_2O_5^- + H_2O \rightarrow Cr_2O_6H^-$ | 184 | 201 | $2 \times 10^{-11}$ | $2.2 \times 10^{-9}$ | 1 |
| (5) $Cr_2O_5^- + H_2O \rightarrow Cr_2O_6H_2^-$ | 184 | 202 | $7 \times 10^{-11}$ | $2.2 \times 10^{-9}$ | 3 |
| $Cr_2O_6^- + H_2O \rightarrow$ no reaction | 200 | no reaction[e] | | $2.2 \times 10^{-9}$ | |
| $Cr_2O_6H_2^- + H_2O \rightarrow$ no reaction | 202 | no reaction[e] | | $2.2 \times 10^{-9}$ | |
| $Cr_2O_6H_4^- + H_2O \rightarrow$ no reaction | 204 | no reaction[e] | | $2.2 \times 10^{-9}$ | |

[a] Units are $cm^3$ $molecule^{-1}$ $s^{-1}$. [b] Rate constants were calculated from kinetic modeling. [c] Average dipole orientation collision constant. [d] $k_{individual}$ as a percentage of $k_{ADO}$. [e] Reaction rate constants $<1 \times 10^{-12}$.

the reparametrized average dipole orientation collision constant ($k_{ADO}$).[69] The slow reactivity was reminiscent of previous studies of $AlO_2^-$ and $SiO_2^-$, both of which reacted very slowly with water despite the fact that the ions were significantly undercoordinated.[41,42]

The other three ions that comprise the $Cr_1O_yH_z^-$ envelope were not observed to undergo any reaction with $H_2O$. We estimated that the slowest reactions observable in the IT-SIMS used in this study had rate constants on the order of $1 \times 10^{-12}$ $cm^3$ $molecule^{-1}$ $s^{-1}$, and therefore, if reactions are occurring, then they must have rate constants less than this value. The failure of $CrO_3^-$ to react contrasted sharply with the behavior of ions in the $Cr_2O_yH_z^-$ envelope, some of which also have trigonally coordinated Cr centers. $CrO_3^-$ enjoys considerable stability compared with other gas-phase Cr oxyanions,[72] and this conclusion was supported by subsequent ab initio calculations. The stability was in accord with the finding that $CrO_3^-$ is normally the most abundant ion in the negative SIMS spectra of chromium oxide-bearing surfaces.[27]

**$Cr_2O_yH_z^-$ + $H_2O$.** Undercoordinated ions in the $Cr_2O_yH_z^-$ envelope were more reactive than the $Cr_1$ species. At short reaction times, $Cr_2O_4^-$ reacted with $H_2O$ to form the monohydrated species $Cr_2O_5H_2^-$ (*m/z* 186) (Figure 2, reaction 1). At longer times, $Cr_2O_6H_4^-$ and $Cr_2O_6H_3^-$ were observed. The mass spectra also showed lower abundance $Cr_2O_6^-$ (*m/z* 200) and $CrO_3^-$ (*m/z* 100), which were determined to be due to reaction with $O_2$ in the IT-SIMS, and are the subject of a second paper. The kinetic profiles are in good agreement with a reaction sequence in which the reactant at *m/z* 168 was transformed to the intermediate at *m/z* 186, which then went on to form product ions at *m/z* 204 and 203 via parallel reactions (Figure 3). Thus, $Cr_2O_5H_2^-$ underwent addition to form $Cr_2O_6H_4^-$ (reaction 3) and OH abstraction to form $Cr_2O_6H_3^-$ (reaction 2).

$$Cr_2O_4^- + H_2O \xrightarrow{k_1} Cr_2O_5H_2^- \quad (1)$$

$$Cr_2O_5H_2^- + H_2O \xrightarrow{k_2} Cr_2O_6H_3^- + H \quad (2)$$

$$Cr_2O_5H_2^- + H_2O \xrightarrow{k_3} Cr_2O_6H_4^- \quad (3)$$

Two other conclusions may be drawn: First, $Cr_2O_4^-$ does not appear to participate in radical abstraction reactions, which may suggest that this ion has predominantly even-electron character in the valence orbitals. We have noted that odd-electron species such as $SiO_2^-$ and $SiO_3^-$ tend to participate primarily in radical abstraction reactions, but that even-electron species such as

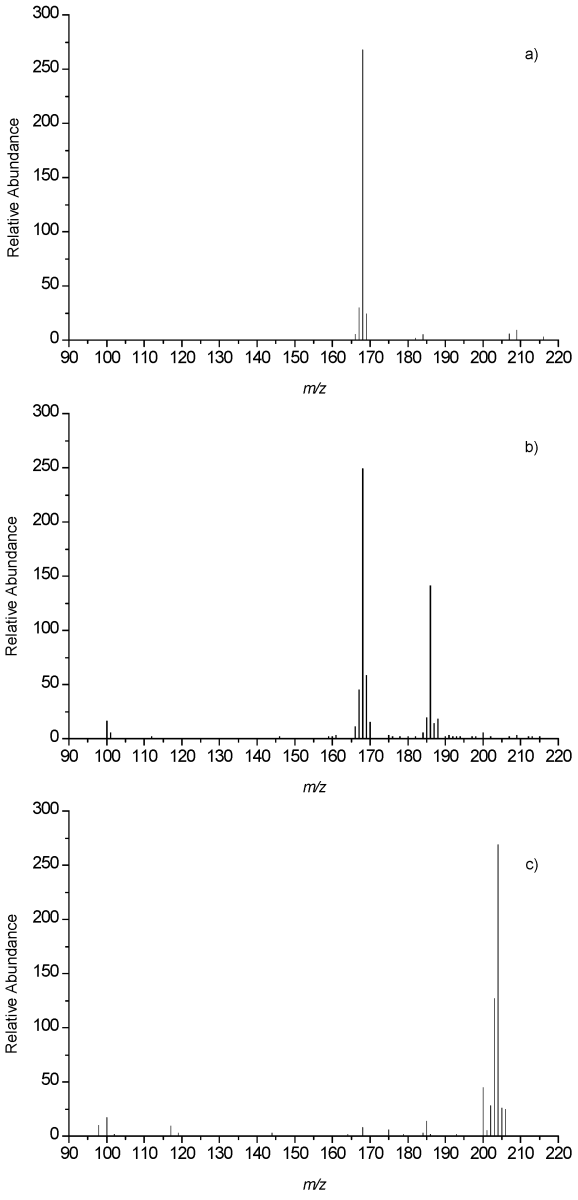


**Figure 2.** Anion IT-SIMS spectra from association reaction of isolated $Cr_2O_4^-$ (*m/z* 168) with a $H_2O$ pressure of $1.3 \times 10^{-6}$ Torr. Reaction times: (a) 0 ms, (b) 80 ms, (c) 1500 ms.

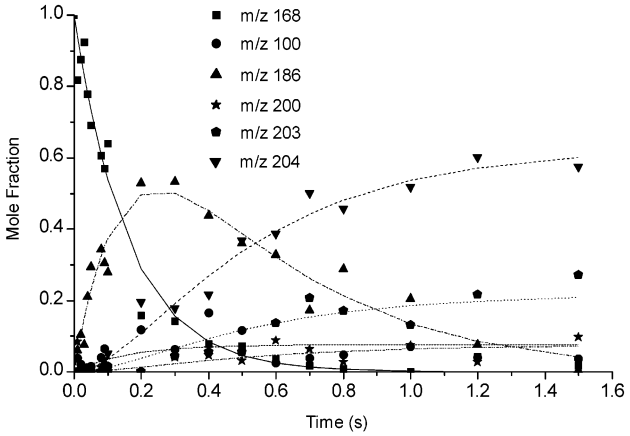


**Figure 3.** Kinetic profile and selected ion channel data for parent ion $Cr_2O_4^-$ (*m*/*z* 168) reaction with excess $H_2O$.

$SiO_3H^-$ and $AlO_2^-$ do not.[41,42,73] The second conclusion is that the $Cr_2O_6H_z^-$ product ions do not participate in further reactions with water under the vacuum conditions of the IT-SIMS.

The individual rate constants for reactions 1−3 were estimated using the ALS method for the model defined by reactions 1−3. The rate constant for reaction 1 was determined to be $1 \times 10^{-10}$ cm$^3$ molecule$^{-1}$ s$^{-1}$, which made the reaction about 7% efficient compared with the $k_{ADO}$ of $2 \times 10^{-9}$ cm$^3$ molecule$^{-1}$s$^{-1}$ (Table 1). Reaction efficiencies for reactions 2 and 3 were substantially lower (0.6% and 2%, respectively), which is in accord with the fact that, as the average coordination of the metal increases, reactivity decreases.[32,41,42,60,74−76]

$Cr_2O_5^-$ (*m*/*z* 184) also reacted with $H_2O$ forming $Cr_2O_6H^-$ (*m*/*z* 201, reaction 4) and $Cr_2O_6H_2^-$ (*m*/*z* 202, reaction 5) (Figure 4). The kinetic profile (Figure 5) indicated that reactions 4 and 5 proceeded in parallel,

$$Cr_2O_5^- + H_2O \xrightarrow{k_4} Cr_2O_6H^- + H \quad (4)$$

$$Cr_2O_5^- + H_2O \xrightarrow{k_5} Cr_2O_6H_2^- \quad (5)$$

and an evaluation of the rate constants revealed efficiencies that were 1% and 3%, respectively. These values were comparable to those determined for the reactions of $Cr_2O_5H_2^-$ with $H_2O$, and indicated that the presence of H atoms on the periphery of the molecule had little influence on the approach of the incoming $H_2O$. This supports the nucleophilic mechanism indicated by the ab initio calculations (vide infra).

As noted previously, as the average coordination of the Cr centers increased, reactivity decreased: $H_2O$ did not appear to react with any of the $Cr_2O_6H_z^-$ ($z = 0-4$) ions.

**Ab Initio Calculations.** Further understanding of the $Cr_xO_yH_z^-$ + $H_2O$ reactions was generated using ab initio calculations at the Hartree−Fock level of theory. One limitation of this approach was that reaction coordinates were only calculated for ground-state molecules: in actuality, the ions in the trap occupied a range of vibrational states and kinetic energies, which implied that the reactivity observed could be different from what was calculated. Nevertheless, the calculations complemented the experimental studies because they provided probable low-energy structures and relative thermodynamic values for reactants and products. The computational results should be in qualitative accord with the experimental observations.

For the reactions of $CrO_2^-$, $CrO_3^-$, $CrO_4^-$, and $CrO_4H^-$ with $H_2O$, realistic transition states could not be located which connected them with products ($CrO_3H_2^-$, $CrO_4H_2^-$, $CrO_5H_2^-$, and $CrO_5H_3^-$, respectively). In the case of $CrO_3^-$, high barriers

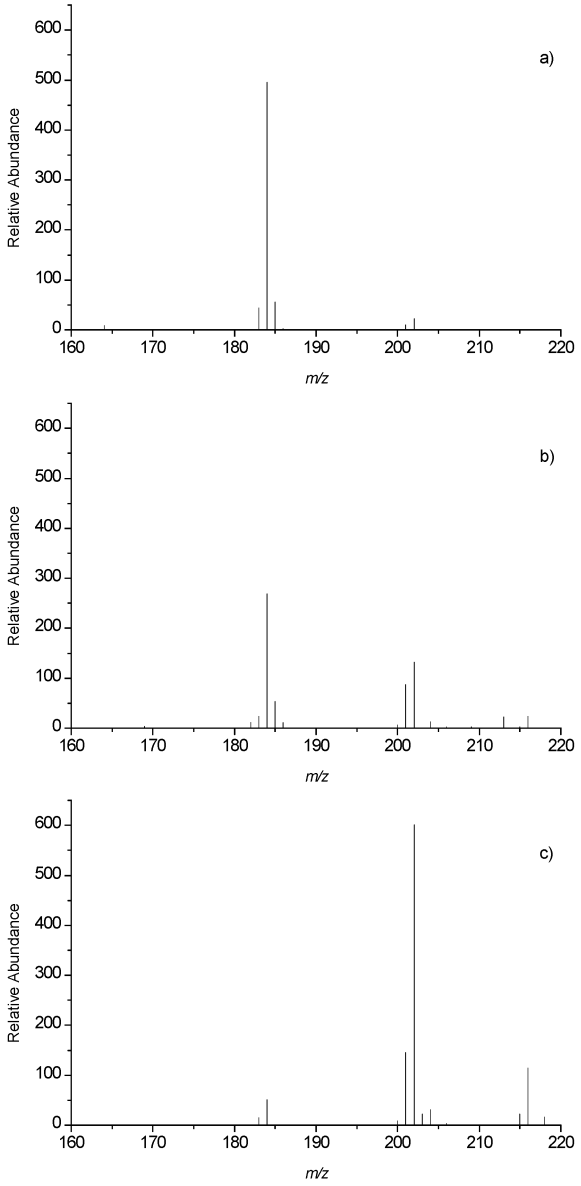


**Figure 4.** Anion IT-SIMS spectra from association reaction of isolated $Cr_2O_5^-$ (*m*/*z* 184) with a $H_2O$ pressure of $1.3 \times 10^{-6}$ Torr. Reaction times: (a) 0 ms, (b) 100 ms, (c) 600 ms.

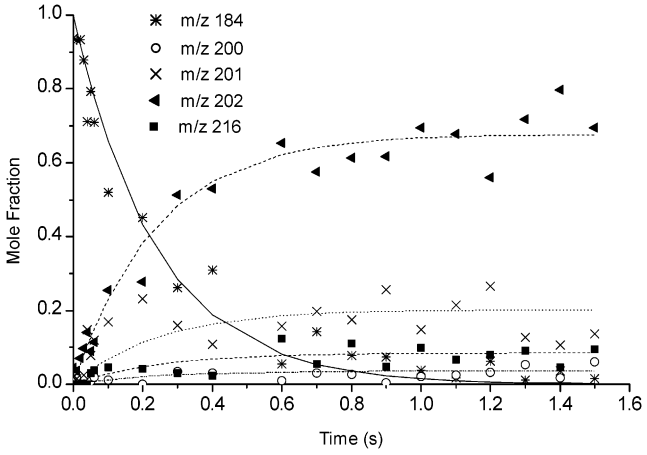


**Figure 5.** Kinetic profile and selected ion channel data for parent ion $Cr_2O_5^-$ (*m*/*z* 184) reaction with excess $H_2O$.

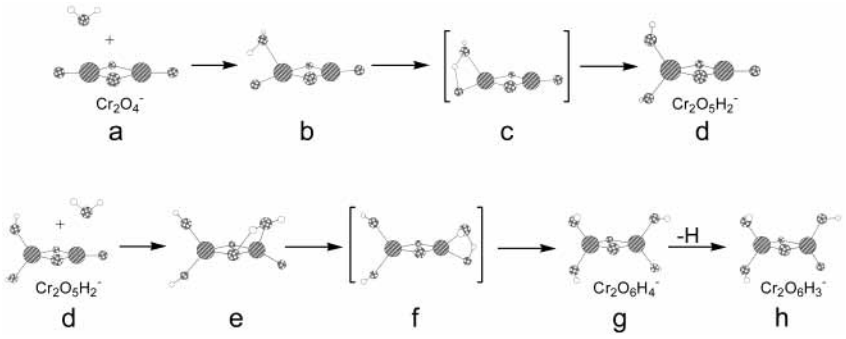


**Figure 6.** Ab initio structures calculated for the reactions of (1) $Cr_2O_4^- + H_2O \rightarrow Cr_2O_5H_2^-$ and (2, 3) $Cr_2O_5H_2^- + H_2O \rightarrow Cr_2O_6H_4^-$ and $Cr_2O_6H_3^-$.

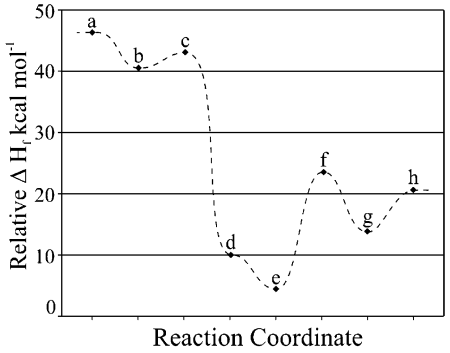


**Figure 7.** Potential energy surface (PES) for the reactions $Cr_2O_4^- + H_2O \rightarrow Cr_2O_5H_2^-$ and $Cr_2O_5H_2^- + H_2O \rightarrow Cr_2O_6H_4^- \rightarrow Cr_2O_6H_3^- + H$. The associated structures **a**−**h** are shown in Figure 6.

prohibited formation of addition adducts. For $CrO_2^-$, $CrO_4^-$, and $CrO_4H^-$, stable products could not be identified.

When $Cr_2O_4^-$ was modeled, a cyclic structure containing a rhombic $Cr_2O_2$ moiety with two pendant O atoms emerged as the lowest energy structure (Figure 6). This result was consistent with the recent DFT calculations of Xiang and co-workers,[77] who concluded that, for neutral $Cr_xO_y$ species, the rhombic structure was more stable than any alternative by nearly 3 eV/molecule. The initial $[Cr_2O_4 + H_2O]^-$ adduct (**b**) was formed by an exothermic process (∼6 kcal mol$^{-1}$) in which the water O atom approached a Cr center, i.e., a nucleophilic attack on the Cr. This mechanism was very different from that calculated for the addition of $H_2O$ with $AlO_2^-$ and $SiO_2^-$: in these reactions, the initially formed adduct was a H-bound structure, and the (Al or Si)−O bond was not formed until after the formation of the H-bound adduct.

After formation of **b**, a H atom was transferred to the *gem* O atom, producing a *gem*-dihydroxy structure for $Cr_2O_5H_2^-$ (**d**) via a low-lying transition state (**c**). The overall reaction was calculated to be about 36 kcal mol$^{-1}$ exothermic (Figure 7). The poor reaction efficiency suggested a steric impediment to the reaction (instead of a transition-state barrier): this may support the proposed mechanism involving nucleophilic attack by water in the formation of the initial adduct **b**, which may be inefficient because end-on or side-on approaches would be expected to result in repulsion by the high electron density associated with the pendant O atoms of the $Cr_2O_4^-$ reactant (**a**).

Once formed, **d** reacted with a second $H_2O$, which approached the remaining trigonally coordinated Cr atom to form the $[Cr_2O_5H_2 + H_2O]^-$ adduct (**e**). Consistent with the initial $H_2O$ addition reaction, this process was ∼6 kcal mol$^{-1}$ exothermic. Transition to the bis-dihydroxy $Cr_2O_6H_4^-$ product (**g**) required surmounting a transition-state barrier that was ∼19 kcal mol$^{-1}$ (**f**). Furthermore, formation of **g** was ∼4 kcal mol$^{-1}$ endothermic relative to the reactants **d** + $H_2O$, and **g** was found to be ∼9 kcal mol$^{-1}$ above the adduct **e**. The energetic considerations suggested that hydrogen rearrangement of **e** resulting in formation of **g** was probably not occurring: the ions have inadequate kinetic energy,[78] and there was probably ample opportunity for the reactant **d** and/or adduct **e** to dissipate vibrational/rotational energy left over from reaction 1 (**a** → **d**).

The origin of the 19 kcal mol$^{-1}$ transition-state barrier for the conversion of **e** to **g** posed an intriguing question, because the reaction **e** → **f** appeared to be very similar to **b** → **c** in terms of the atoms involved and the overall geometry. However, a comparison of the negative charge densities found on the two reactant ions **a** and **d** showed a lower charge density on the pendant O atom in **d** than was found in **a**, where the higher symmetry in **a** may allow better localization of the charge on the pendant oxygens. Conversely, in **d** the rhombic oxygens ($O_{rhombic}$) carried a higher charge density, which led to formation of a relatively strong H−$O_{rhombic}$ bond (1.61 Å) in **e**. This contrasted with **b**, in which a H−$O_{rhombic}$ bond was not formed. Instead, **b** underwent H rearrangement between two pendant *gem* O atoms via transition state **c**, which required the two *gem* O atoms to rock close to one another. A similar rearrangement in the $[Cr_2O_5H_2 + H_2O]^-$ transition state (**f**) would be energetically more demanding, because the H−$O_{rhomibic}$ bond would have to be broken to enable the water to rock into the transition-state geometry. This may explain the augmented energetic requirements for reaching transition-state **f**.

A surprising result of the calculations was that the relative $\Delta H_f$ calculated for the bis-dihydroxy structure **g** for $Cr_2O_6H_4^-$ was ∼9 kcal mol$^{-1}$ *greater* than that for **e**. This contrasted sharply with the calculations for **b** and **d**, which showed that the $\Delta H_f$ for the *gem*-dihydroxy structure **d** was >30 kcal mol$^{-1}$ *lower* than that of **b**. On the basis of past calculations performed for Al and Si systems, the latter result seems to be typical. The $\Delta H_f$ of the bis-dihydroxy structure **g** may be greater than that of **e** because there is no obvious place to localize charge in **g** (i.e., no pendant O moieties).

The formation of $Cr_2O_6H_3^-$ (**h**) is clearly indicated by the mass spectra, and the kinetic analysis shows that it is formed in parallel with $Cr_2O_6H_4^-$ (Figure 3). Calculations showed that the $\Delta H_f$ of $Cr_2O_6H_3^-$ + H was 11 kcal mol$^{-1}$ endothermic compared with the reactants $Cr_2O_5H_2^- + H_2O$, and if the precursor ion is $Cr_2O_6H_4^-$, then the aforementioned 19 kcal mol$^{-1}$ transition state **f** would have to be surmounted. If this were indeed the reaction pathway, then only those ions having residual vibrational energy from reaction 1 would form the $Cr_2O_6H_3^-$ ion. This explanation would be consistent with the kinetics if the elimination of H were much faster than the bimolecular processes; i.e., slow formation of **g** followed by

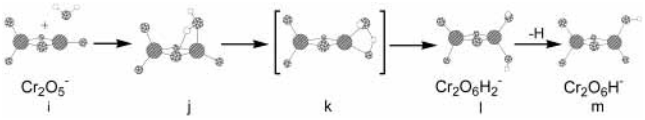


**Figure 8.** Ab initio structures calculated for the reactions (4, 5) $Cr_2O_5^- + H_2O \rightarrow Cr_2O_6H_2^-$ and $Cr_2O_6H^-$. Formulas written under ion structures correspond to stable ions observed in the ion trap.

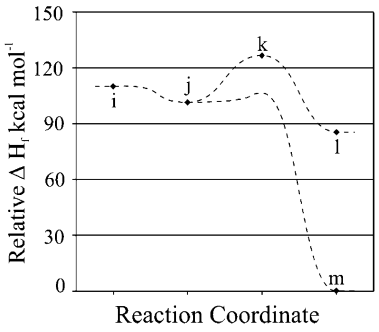


**Figure 9.** PES for the reactions $Cr_2O_5^- + H_2O \rightarrow Cr_2O_6H_2^- \rightarrow Cr_2O_6H^- + H$. The associated structures **i**−**m** are shown in Figure 8.

very fast elimination of H to form **h** from a fraction of **g** would appear as parallel processes in the kinetic plot. Elimination of a H radical from **e** is another possibility that cannot be excluded. No transition state could be identified for expulsion of H from either **e** or **g**.

Ab initio modeling of the reaction of $Cr_2O_5^-$ (**i**) with $H_2O$ resulted in formation of a $[Cr_2O_5 + H_2O]^-$ adduct (**j**) that was about 9 kcal $mol^{-1}$ more stable than the reactants (Figures 8 and 9). This value was very consistent with the exothermicity noted for the formation of the initial adducts **b** and **e**. The calculated structure suggested that adduct **j** likely contained a $H-O_{rhombic}$ hydrogen bond (1.79 Å) which may be a consequence of charge density localized on the rhombic O atom (similar to **e**). From this point on the potential energy surface calculations suggested that ∼26 kcal $mol^{-1}$ would be required to go to the *gem*-dihydroxy structure **l** via transition state **k**. Since these energetic requirements were unlikely to be met, this reaction does not occur, but adduct **j** was evidently sufficiently stable to survive scan out and detection, thereby accounting for the ion observed at *m*/*z* 202.

Even though the height of transition state **k** prohibits formation of the *gem*-dihydroxy structure **l** for $Cr_2O_6H_2^-$, it was noteworthy that the $\Delta H_f$ for **l** is ∼15 kcal $mol^{-1}$ lower than that of **j**. Thus, the order of stability was reversed compared with the $\Delta H_f$ order for the *gem*-dihydroxy and adduct structures in the $Cr_2O_6H_4^-$ system (structures **e** and **g**). The difference may be due to the fact that, in the $Cr_2O_6H_2^-$ system, there are pendant O atoms where negative charge can be stabilized. This is consistent with the interpretation offered in explanation of the relatively high $\Delta H_f$ calculated for **g**; viz., absence of pendant O atoms for charge stabilization produces higher $\Delta H_f$ values.

An ab initio pathway for the elimination of H to form $Cr_2O_6H^-$ (*m*/*z* 201) was not identified. Since the kinetic analysis indicated that formation of $Cr_2O_6H^-$ occurred in parallel with the addition, involvement of a third neutral is unlikely. Instead, this suggests that vibrationally excited $Cr_2O_6H_2^-$ may eliminate H in a unimolecular fashion, at a rate that is much faster than that of the bimolecular addition. In this case, the appearance of $Cr_2O_6H^-$ and $Cr_2O_6H_2^-$ would appear to be parallel reactions. Since formation of the *gem*-dihydroxy structure **l** is unlikely, loss of H from **j** was hypothesized. The relative $\Delta H_f$ for the minimized $Cr_2O_6H^-$ structure (**m**) was significantly less than that of the adduct **j**. However, there must be a barrier (not yet identified); otherwise the adduct **j** would not be observed at all.

## IV. Conclusions

The present studies of Cr oxyanion reactions with $H_2O$ showed a wide range of reactivities. All $Cr_1O_yH_z^-$ species were unreactive under the conditions of the ion trap, except for $CrO_2^-$, which underwent a very slow reaction of water addition. This suggested that reactions of small Cr oxyanions with $H_2O$ are not important in the formation of large clusters.[20,21] However, this conclusion was tempered by the observation that these reactions were studied at 310 K (estimated), and rates and reaction channels may be vastly different at higher temperatures typical of a particle or photon impact zone. In contrast to the $Cr_1$ species, the $Cr_2O_yH_z^-$ species reacted slowly with $H_2O$ as long as Cr centers having coordination less than 4 were available. This observation was in general accord with the conclusions of Castleman[74] and Squires[75] regarding the reactivity of undercoordinated metal centers.

The behavior of the undercoordinated $Cr_2O_yH_z^-$ implied that reactive chromium oxide centers require at least two Cr atoms, even if one of the metals does not directly participate in the reaction. This conclusion was similar to that for small Si and Al oxyanions, in that $Si_2$ and $Al_2$ oxyanion species were much more reactive than were $Si_1$ and $Al_1$ species. However, in the reactions of the $Si_2$ and $Al_2$ oxyanions, both metal atoms participated: $H_2O$ addition reactions occurred across the rhombic $M_2O_2$ moieties. In the case of the $Cr_2$ oxyanions, $H_2O$ addition occurs in a geminal fashion.

The approach of the reactant $H_2O$ to the $Cr_2$ oxyanions presents another interesting contrast with the previous studies of the Al and Si oxyanions. In the reactions of the $Cr_2$ oxyanions, $H_2O$ behaves as a nucleophile, and the initial approach involves attack of the $H_2O$ oxygen on the undercoordinated Cr center. Stable hydrogen-bound adducts were not identified by the ab initio calculations, which differed from the behavior modeled for $H_2O$ approach to the Si and Al oxyanions. In the Si and Al examples, the initially formed species was a hydrogen-bound $[M_xO_y + H_2O]^-$ adduct, which then rearranged to produce vicinal dihydroxy products. At present, it is not understood why the Cr oxyanions do not form stable hydrogen-bound adducts, instead preferring to behave as negatively charged electrophiles. However, this computational phenomenon may be in accord with the low reaction efficiencies determined experimentally.

**Acknowledgment.** The funding support of the United States Department of Energy, Environmental Systems Research program, under Contract DE-AC-07-99ID13727 BBWI is gratefully acknowledged. The Ohio University Faculty Fellowship Leave and the Idaho National Engineering and Environmental Laboratory Faculty Leave Fellowship programs are thanked for their financial support. We thank Dr. W. L. Bauer for helpful discussions.

**Supporting Information Available:** IT-SIMS spectra and kinetic profile. This material is available free of charge via the Internet at http://pubs.acs.org.

## References and Notes

(1) Kimbrough, D. E.; Cohen, Y.; Winer, A. M.; Creelman, L.; Mabuni, C. *Crit. Rev. Environ. Sci. Technol.* **1995**, *29*, 1.
(2) Bencko, V. *J. Hyg. Epidimol. Microbiol. Immunol.* **1985**, *29*, 37.
(3) O'Day, P. A. *Rev. Geophys.* **1999**, *37*, 249.

(4) Cary, E. E. Chromium in air, soil, natural waters. In *Biological and Environmental Aspects of Chromium*; Langard, Ed.; Elsevier Biomedical Press: New York, 1982; Vol. 5, p 49.
(5) Evans, L. J. *Environ. Sci. Technol.* **1989**, *23*, 1046.
(6) Jardine, P. M.; Fendorf, S. E.; Mayes, M. A.; Larsen, I. L.; Brooks, S. C.; Bailey, W. B. *Environ. Sci. Technol.* **1999**, *33*, 2939.
(7) Lee, S. Z.; Chang, L. Z.; Ehrlich, R. S. *J. Environ. Sci. Health, Part A* **1999**, *34*, 809.
(8) Lee, S. Z.; Chang, L. Z.; Chen, C. M.; Yang, H. H.; Hu, P. Y. *J. Environ. Sci. Health, Part A* **2001**, *36*, 63.
(9) Pantsar-Kallio, M.; Reinikainen, S.-P.; Oksanen, M. *Anal. Chim. Acta* **2001**, *439*, 9.
(10) Neubauer, K. R.; Johnston, M. V.; Wexler, A. S. *Int. J. Mass Spectrom. Ion Processes* **1995**, *151*, 77.
(11) Struyf, H.; Van Vaeck, L.; Poels, K.; Van Greiken, R. *J. Am. Soc. Mass Spectrom.* **1998**, *9*, 482.
(12) Conradson, S. D. *Appl. Spectrosc.* **1998**, *52*, 252A.
(13) Van Vaeck, L.; Adriaens, A.; Gijbels, R. *Mass Spectrom. Rev.* **1999**, *18*, 1.
(14) Poels, K.; Van Vaeck, L.; Gijbels, R. *Anal. Chem.* **1998**, *70*, 504.
(15) Huo, D.; Kingston, H. M. *Anal. Chem.* **2000**, *72*, 5047.
(16) Aubriet, F.; Maunit, B.; Muller, J.-F. *Int. J. Mass Spectrom.* **2001**, *209*, 5.
(17) Aubriet, F.; Maunit, B.; Muller, J.-F. *Int. J. Mass Spectrom. Ion Processes* **2000**, *198*, 189.
(18) Aubriet, F.; Poleunis, C.; Bertrand, P. *J. Mass Spectrom.* **2001**, *36*, 641.
(19) Aubriet, F.; Muller, J. F. *J. Phys. Chem. A* **2002**, *106*, 6053.
(20) Hachimi, A.; Millon, E.; Poitevin, E.; Muller, J. F. *Analusis* **1993**, *21*, 11.
(21) Hachimi, A.; Poitevin, E.; Krier, G.; Muller, J.-F.; Ruiz-Lopez, M. F. *Int. J. Mass Spectrom. Ion Processes* **1995**, *144*, 23.
(22) Hachimi, A.; Van Vaeck, L.; Poels, K.; Adams, F. C.; Muller, J.-F. *Spectrochim. Acta, Part B* **1998**, *53*, 347.
(23) Van Vaeck, L.; Adriaens, A.; Adams, F. *Spectrochim. Acta, Part B* **1998**, *53*, 367
(24) Aubriet, F.; Maunit, B.; Courrier, B.; Muller, J.-F. *Rapid Commun. Mass Spectrom.* **1997**, *11*, 1596.
(25) Aubriet, F.; Maunit, B.; Muller, J.-F. *Int. J. Mass Spectrom.* **2000**, *198*, 213.
(26) Hachimi, A.; Poitevin, E.; Krier, G.; Muller, J. F.; Pironon, J.; Klein, F. *Analusis* **1993**, *21*, 77.
(27) Benninghoven, A. *Surf. Sci.* **1973**, *35*, 427.
(28) Plog, C.; Wiedmann, L.; Benninghoven, A. *Surf. Sci.* **1977**, *67*, 565.
(29) Van Stipdonk, M. J.; Justes, D. R.; Force, C. M.; Schweikert, E. A. *Anal. Chem.* **2000**, *72*, 2468.
(30) Frenkel, A. I.; Hills, C. W.; Nuzzo, R. G. *J. Phys. Chem. B* **2001**, *105*, 12689.
(31) Zachara, J. M.; McKinley, J. P. *Aquat. Sci.* **1993**, *44*, 250.
(32) Dinca, A.; Davis, T. P.; Fisher, K. J.; Smith, D. R.; Willett, G. D. *Int. J. Mass Spectrom. Ion Processes* **1999**, *183*, 73.
(33) Dietze, H.-J.; Becker, S. *Int. J. Mass Spectrom. Ion Processes* **1988**, *82*, 47.
(34) Finke, R. G.; Droege, M. W.; Cook, J. C.; Suslick, K. S. *J. Am. Chem. Soc.* **1984**, *106*, 5750.
(35) Maleknia, S.; Brodbelt, J.; Pope, K. *J. Am. Soc. Mass Spectrom.* **1991**, *2*, 212.
(36) Truenbenbach, C. S.; Houalla, M.; Hercules, D. M. *J. Mass Spectrom.* **2000**, *35*, 1121.
(37) Volkening, J.; Walczyk, T.; Heumann, K. G. *Int. J. Mass Spectrom. Ion Processes* **1991**, *105*, 147.
(38) Weiser, P.; Wurster, R.; Seiler, H. *Atmos. Environ.* **1980**, *14*, 485.
(39) Sigsworth, S. W.; Castleman, A. W. *J. Am. Chem. Soc.* **1992**, *114*, 10471.
(40) Fokkens, R. H.; Gregor, I. K.; Nibbering, N. M. M. *Rapid Commun. Mass Spectrom.* **1991**, *5*, 368.
(41) Groenewold, G. S.; Scott, J. R.; Gianotto, A. K.; Hodges, B. D. M.; Kessinger, G. F.; Benson, M. T.; Wright, J. B. *J. Phys. Chem. A* **2001**, *105*, 9681.
(42) Scott, J. R.; Groenewold, G. S.; Gianotto, A. K.; Benson, M. T.; Wright, J. B. *J. Phys. Chem. A* **2000**, *104*, 7079.
(43) Bartmess, J. E.; Georgiadis, R. M. *Vacuum* **1983**, *33*, 149.
(44) Groenewold, G. S.; Appelhans, A. D.; Ingram, J. C. *J. Am. Soc. Mass Spectrom.* **1998**, *9*, 35.
(45) Van Stipdonk, M. J.; Santiago, V.; Schweikert, E. A. *J. Mass Spectrom.* **1999**, *34*, 554.
(46) Groenewold, G. S.; Delmore, J. E.; Olson, J. E.; Appelhans, A. D.; Ingram, J. C.; Dahl, D. A. *Int. J. Mass Spectrom. Ion Processes* **1997**, *163*, 185.
(47) Kelley, P. E. (Teledyne CME). Mass spectrometry method using notch filter. U.S. Patent, 1992.
(48) Todd, J. F. J. Practical Aspects of Ion Trap Mass Spectrometry. In *Practical Aspects of Ion Trap Mass Spectrometry*; March, R. E., Todd, J. F. J., Eds.; CRC Press: New York, 1995; Vol. 1, p 4.
(49) Schmidt, M. W.; Baldridge, K. K.; Boatz, J. A.; Elbert, S. T.; Gordon, M. S.; Jensen, J. H.; Koseki, S.; Matsunaga, N.; Nguyen, K. A.; Su, S. J.; Windus, T. L.; Dupuis, M.; Montgomery, J. A. *J. Comput. Chem.* **1993**, *14*, 1347.
(50) Cramer, C. J.; Truhlar, D. G. *Science* **1992**, *256*, 213.
(51) Gonzalez, C.; Schlegel, H. B. *J. Chem. Phys.* **1989**, *90*, 2154.
(52) Møller, C.; Plesset, M. S. *Phys. Rev.* **1934**, *46*, 618.
(53) Cundari, T. R.; Matsunaga, N.; Moody, E. W. *J. Phys. Chem.* **1996**, *100*, 6475.
(54) Low, J. J.; Goddard, W. A. *J. Am. Chem. Soc.* **1986**, *108*, 6115.
(55) Cundari, T. R.; Snyder, L. A.; Yoshikawa, A. *J. Mol. Struct.: THEOCHEM* **1998**, *425*, 13.
(56) Rappe, A. K. *Organometallics* **1990**, *9*, 466.
(57) Benson, M. T.; Cundari, T. R. *Inorg. Chim. Acta* **1997**, *259*, 91.
(58) Rappe, A. K. *J. Am. Chem. Soc.* **1987**, *109*, 5605.
(59) Musaev, D. G.; Morokuma, K.; Koga, N.; Nguyen, K. A.; Gordon, M. S.; Cundari, T. R. *J. Phys. Chem.* **1993**, *97*, 11435.
(60) Combariza, M. Y.; Vachet, R. W. *J. Am. Soc. Mass Spectrom.* **2002**, *13*, 813.
(61) Baer, T.; Hase, W. L. *Unimolecular Reaction Dynamics*; Oxford University Press: New York, 1996.
(62) Roberge, W.; Dalgarno, A. *Astrophys. J.* **1982**, *255*, 489.
(63) Weishaar, J. C. *Acc. Chem. Res.* **1993**, *26*, 213.
(64) Harrington, P. B.; Gianotto, A. K.; Hodges, B. D. M.; Groenewold, G. S. Manuscript in preparation.
(65) Windig, W.; Guilment, J. *Anal. Chem.* **1991**, *63*, 1425.
(66) de Juan, A.; Maeder, M.; Martinez, M.; Tauler, R. *Chemom. Intell. Lab. Syst.* **2000**, *54*, 123.
(67) de Juan, A.; Maeder, M.; Martinez, M.; Tauler, R. *Anal. Chim. Acta* **2001**, *442*, 337.
(68) Nelder, J. A.; Mead, R. A. *Comput. J.* **1965**, *7*, 308.
(69) Su, T.; Chesnavich, W. J. *J. Chem. Phys.* **1982**, *76*, 5183.
(70) Goeringer, D. E.; McLuckey, S. A. *Int. J. Mass Spectrom. Ion Processes* **1998**, *177*, 163.
(71) Gronert, S. *J. Am. Soc. Mass Spectrom.* **1998**, *9*, 845.
(72) Van Stipdonk, M. J.; Justes, D. R.; Schweikert, E. A. *Int. J. Mass Spectrom.* **2000**, *203*, 59.
(73) Groenewold, G. S.; Hodges, B. D. M.; Scott, J. R.; Gianotto, A. K.; Appelhans, A. D.; Kessinger, G. F.; Wright, J. B. *J. Phys. Chem. A* **2001**, *105*, 4059.
(74) Zemski, K. A.; Justes, D. R.; Castleman, J., A. W. *J. Phys. Chem. B* **2002**, *106*, 6136.
(75) Squires, R. R. *Chem. Rev.* **1987**, *87*, 623.
(76) Gibson, J. K.; Haire, R. G. *J. Alloys Compd.* **2001**, *322*, 143.
(77) Xiang, K.-h.; Pandey, R.; Recio, J. M.; Francisco, E.; Newsam, J. M. *J. Phys. Chem. A* **2000**, *104*, 990.
(78) Jackson, G. P.; King, F. L.; Goeringer, D. E.; Duckworth, D. C. *J. Phys. Chem. A* **2002**, *106*, 7788.